

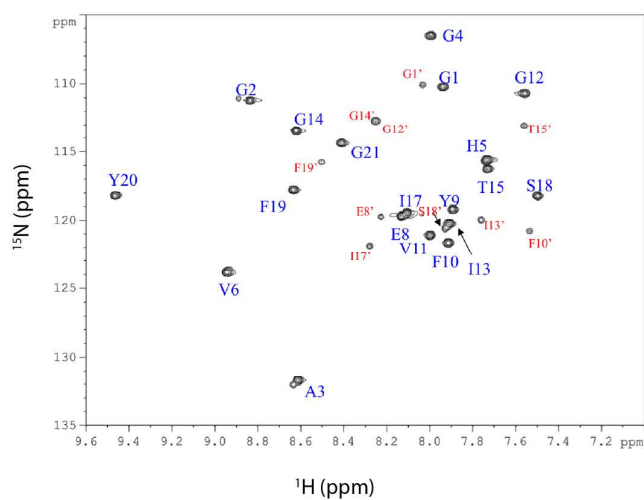
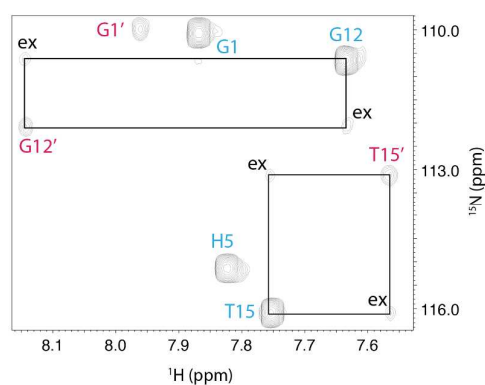
## **Structural basis for natural product selection and export by bacterial ABC transporters**

Maria Romano <sup>1,2,#</sup>, Giuliana Fusco <sup>1,#</sup>, Hassanul G. Choudhury <sup>1,2</sup>, Shahid Mehmood <sup>3</sup>,  
Carol V. Robinson <sup>3</sup>, Séverine Zirah <sup>4</sup>, Julian D. Hegemann <sup>5,6,†</sup>, Ewen Lescop <sup>7</sup>, Mohamed  
A. Marahiel <sup>5</sup>, Sylvie Rebuffat <sup>4</sup>, Alfonso De Simone <sup>1</sup>, Konstantinos Beis <sup>1,2,\*</sup>

**Supplementary Table 1.** Backbone Carbon Chemical Shifts for Pro residues (ppm).

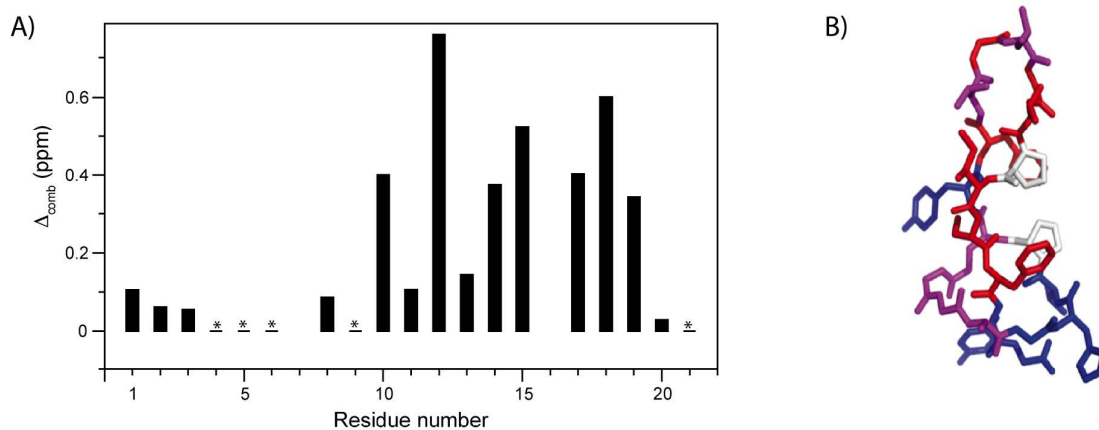
Chemical shift values in red are characteristics of prolines involved in *cis* X-Pro peptide bonds

	C $\alpha$	C $\beta$	CO
7Pro <sup>a</sup>	63.25	31.91	176.4
7Pro <sup>b</sup>	63.74	31.99	176.6
16Pro <sup>a</sup>	63.92	32.23	176.6
16Pro <sup>b</sup>	62.67	34.31	176.0

**a****b**

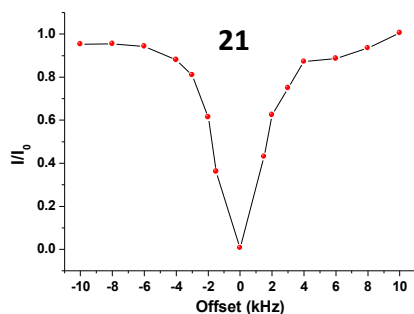
**Supplementary Figure 1.** MccJ25 NMR spectra. a)  $^{15}\text{N}$  HSQC spectrum of  $^{15}\text{N}$ -labeled MccJ25. The crosspeaks are labelled according to their amino-acid number with the labels corresponding to the major and minor forms colored in blue and red respectively. The spectrum was collected at 298K at 950  $^1\text{H}$  MHz frequency. b)  $^{15}\text{N}$  HSQC-based ZZ-exchange spectroscopy highlighting for residues G12 and T15 the exchange between the two conformations. Crosspeaks labelled *ex* are not visible in the  $^{15}\text{N}$  HSQC spectrum and revealed in the ZZ-exchange experiments the interconversion between the two forms during the mixing time (1 s). This experiment confirmed the assignment of the minor form and unambiguously demonstrated that the two observed conformations are exchanging with an

exchange rate at the second timescale. The spectrum was collected at 318K at 950 MHz  $^1\text{H}$  frequency.

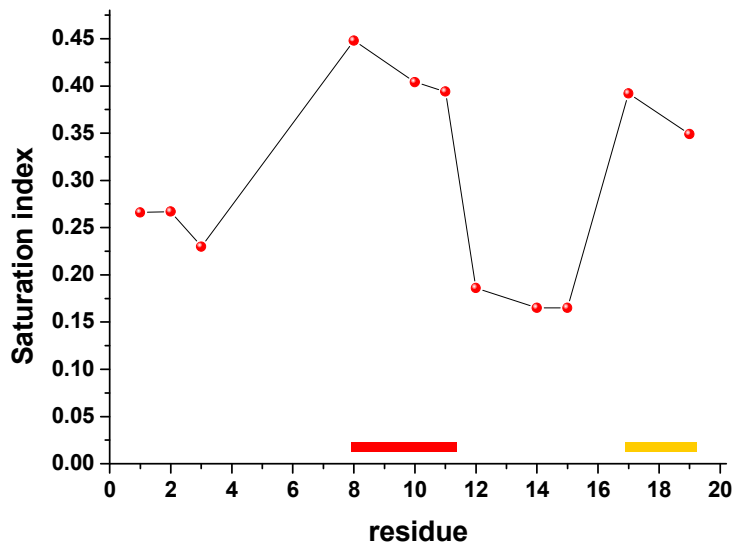


**Supplementary Figure 2.** a) Combined  $^1\text{H}/^{15}\text{N}$  chemical shift difference between the major and minor forms of MccJ25 plotted versus the amino acid number. Residues for which no minor form was detectable are labelled with a star, indicating that the chemical shifts for these residues are indistinguishable in the two forms. b) The chemical shift perturbation is plotted on MccJ25 structure with the most perturbed residues ( $\Delta_{\text{comb}} > 0.3$ ) colored in red, the less perturbed residues ( $\Delta_{\text{comb}} < 0.03$ ) in blue and the other ( $0.05 < \Delta_{\text{comb}} < 0.3$ ) colored in magenta. No data are available for proline residues that are colored white. This figure highlights that the strongest perturbations are visible in the loop region and are centered around P16.

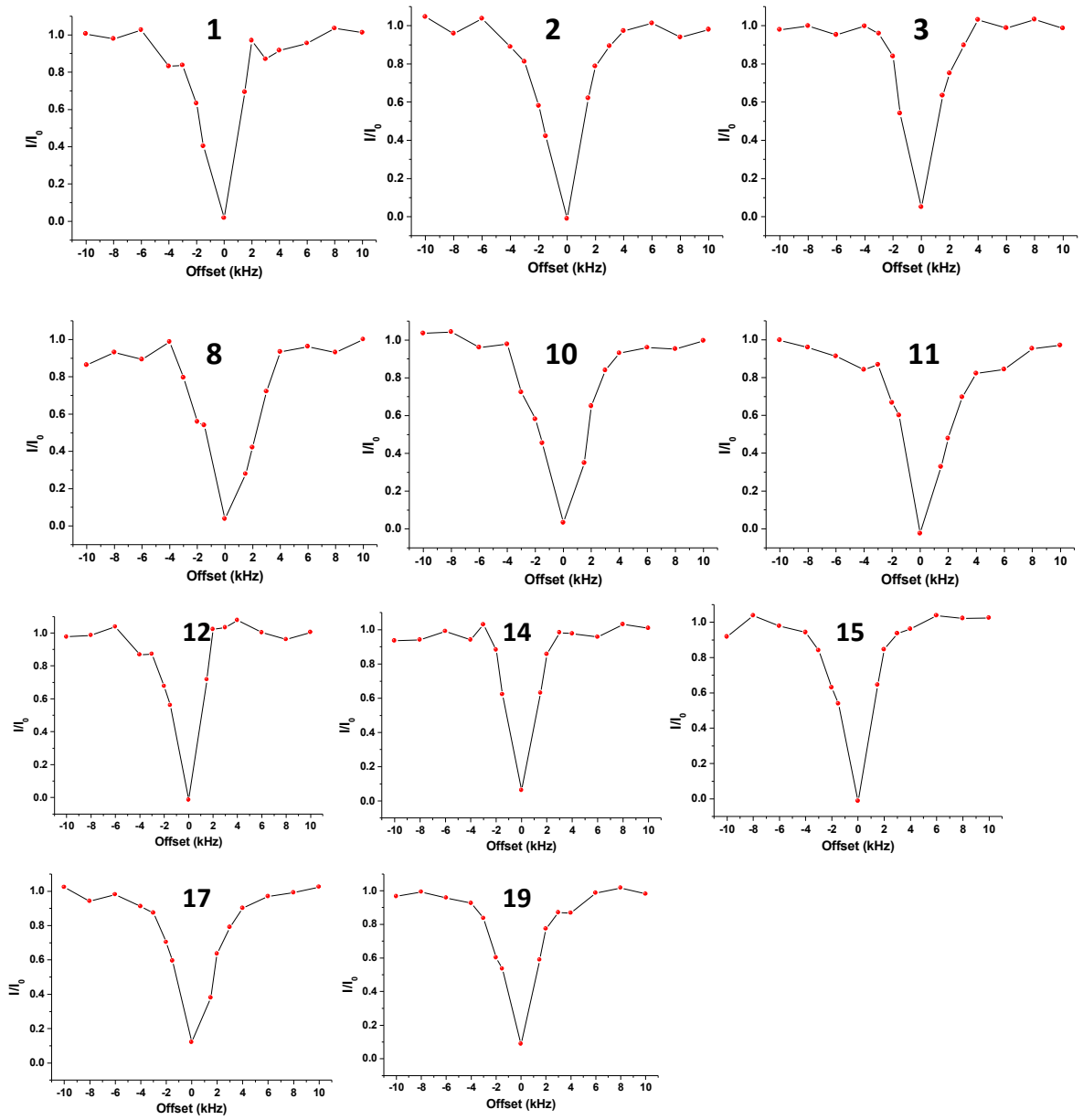




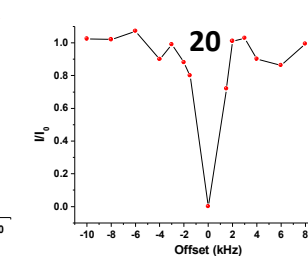
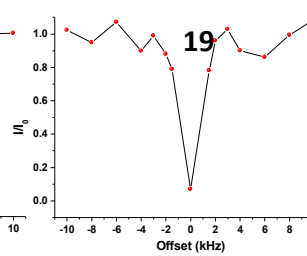
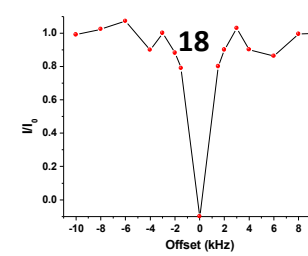
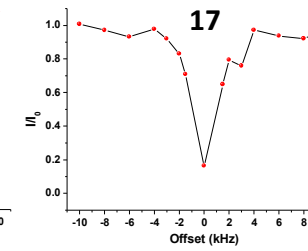
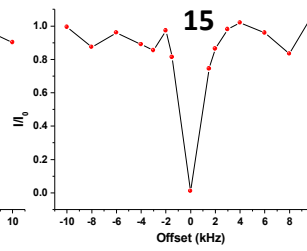
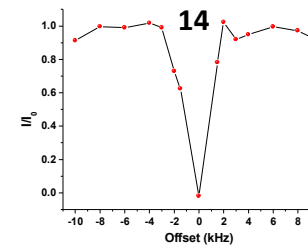
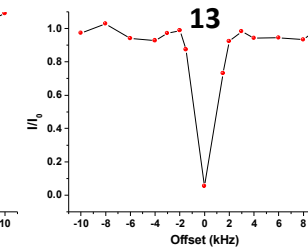
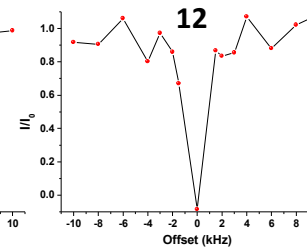
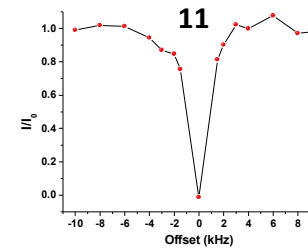
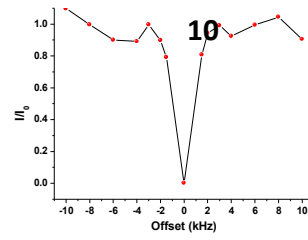
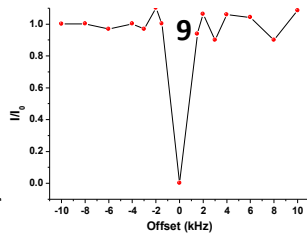
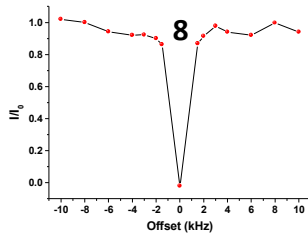
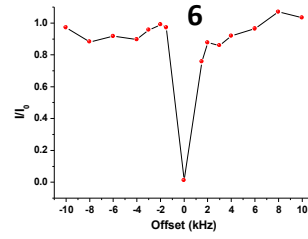
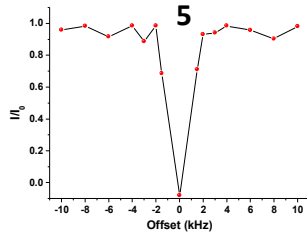
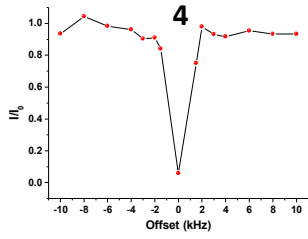
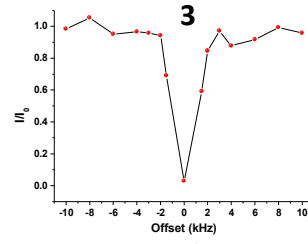
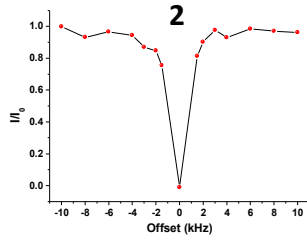
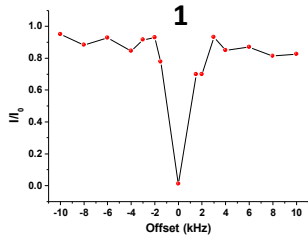
**Supplementary Figure 3.** Saturation profiles in each residue of MccJ25 measured in CEST experiments with McjD embedded in bicelles. The data relative to the main structural state of MccJ25 are reported. CEST measurements were based on  $^1\text{H}$ - $^{15}\text{N}$  HSQC experiments by applying constant wave saturation of 500 Hz in the  $^{15}\text{N}$  channel. A of large offsets was employed (-10, -8, -6, -4, -3, -2, -1.5, 0, 1.5, 2, 3, 4, 6, 8 and 10 kHz), resulting in CEST profiles of symmetric shape. An additional spectrum, saturated at -100 kHz was recorded as reference.

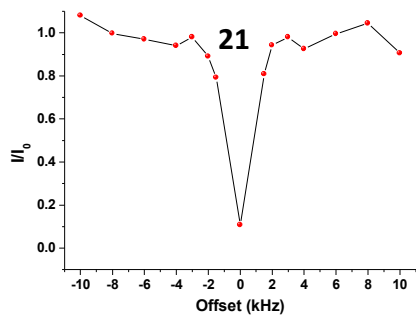


**Supplementary Figure 4.** Saturation index (see METHODS) derived from the analysis of the CEST profiles corresponding to the second conformational state of MccJ25. As in the case of the principal conformational state of MccJ25 (Figure 2e), the data indicate a primary (marked in red) and a secondary (marked in yellow) region experiencing high saturation transfer.

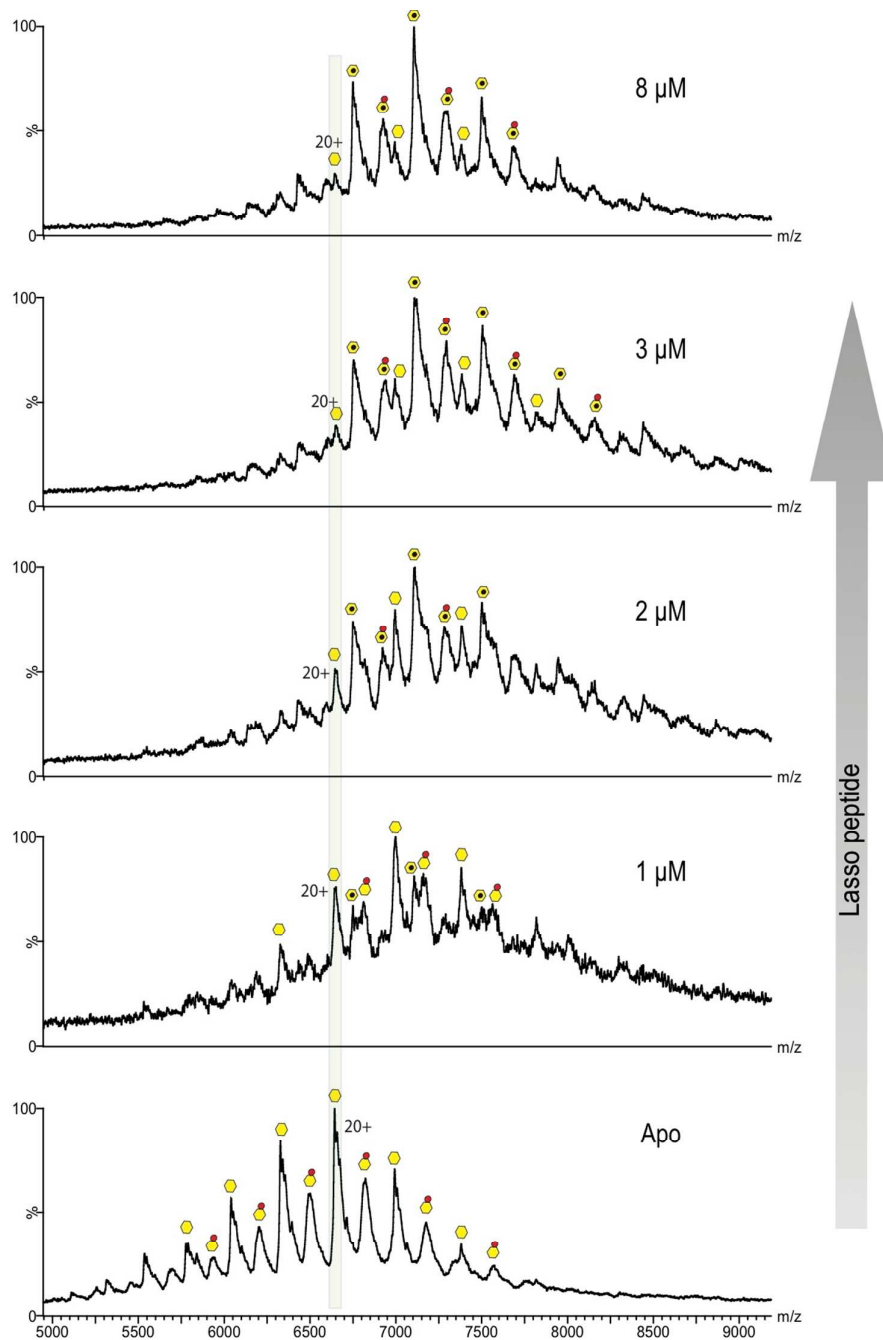


**Supplementary Figure 5.** Saturation profiles in each residue of MccJ25 measured in CEST experiments with McjD embedded in bicelles. The data relative to the secondary structural state of MccJ25 are reported.



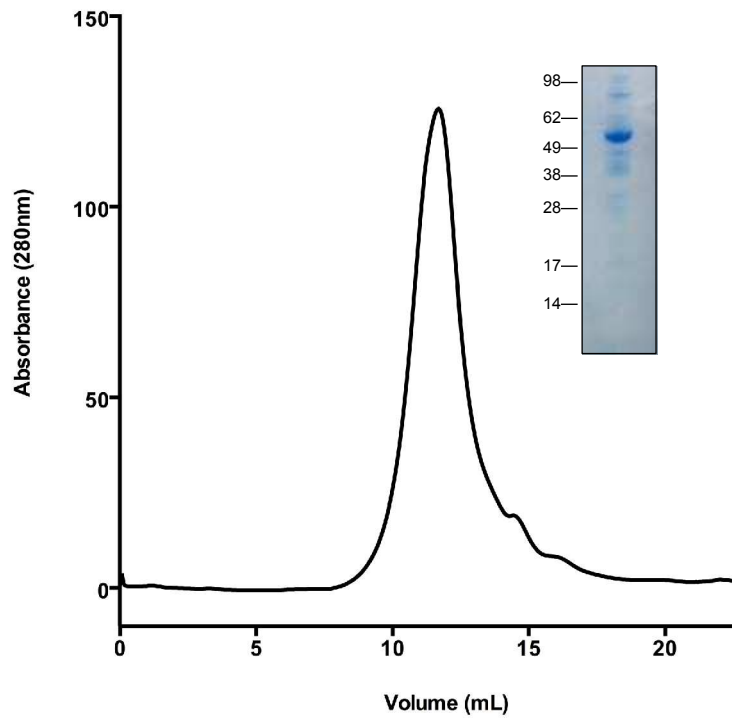


**Supplementary Figure 6.** Saturation profiles in each residue of MccJ25 measured in CEST experiments with bicelles. The data relative to the main structural state of MccJ25 are reported.

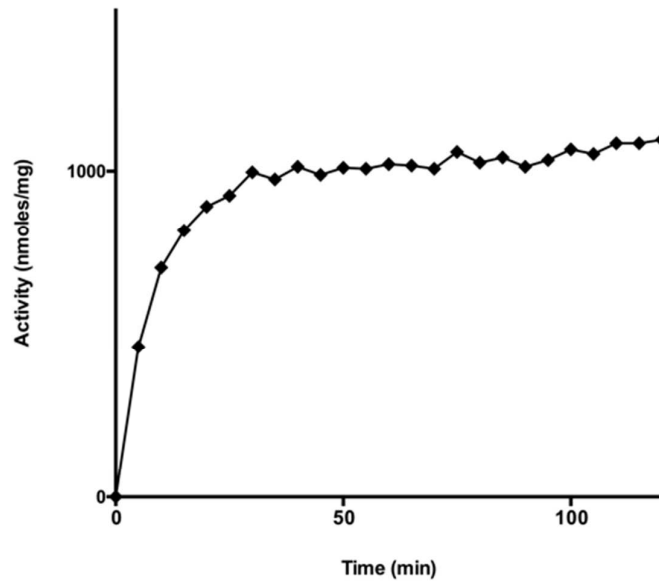


**Supplementary Figure 7.** Mass spectra of apo McjD protein and in complex with varied concentration of MccJ25 show formation of adducts peaks for all charge states. The intensity of the complex peak charge states are increased as a result of increase in peptide concentration. Apo protein, LPS-bound, MccJ25 bound and LPS, MccJ25 bound adduct peaks are labelled with the same legends used for Figure 3c.

**a**



**b**

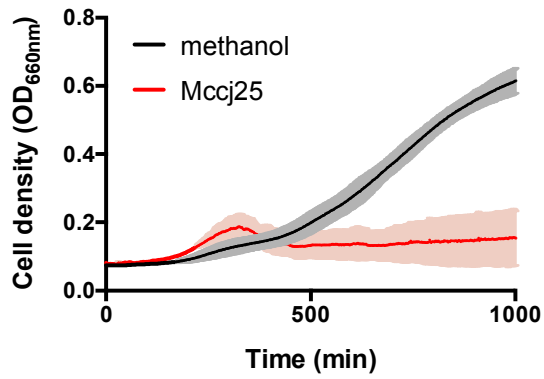


**c**

1 MALPIRNAGL PARSRIDMKL AALRSLADV V RLMVDKETKA RKL**LIVAGVLI**  
51 **EALTSAFMLL** **GPLALKLAVD** **EMSR**AQFDAA KAAVDIVLFA VLWSASAVSS  
101 IALLAYTGKI **VHATSNTLLR** **RALHAQLPAL** **ASRASSDSGY** **VQGLLERLPY**  
151 **SLQVIIEGVL** **WKIAPVAIQL** VVALALIALL VPLRYAAILF AVLAAYFVFS  
201 HLSAEQYENS AATTNHAAGE LSAALGDVLA NAPR**VVYNGA** **VPREIDYVAA**  
251 RADARLDVNW RRSWLLTRAA AYQYGIIALG MAAMFALCVR DIAAHRITLG  
301 DFMLLQTYVL QFALPLGAYG FVLR**QAGAAL** **ANVREALAIA** PR**AGGGDGDG**  
351 **GALAQPRPGG** **SAAHIAVRRL** AFRRAGRFAI **EPMSFDLPAG** **SYTAIVGHNG**  
401 **SGKSTLAKIV** **AGLLPPDEGG** **VAYDGVLDYG** **VAGDARHRFA** **LYVPQDVALL**  
451 **NRSLRENVRY** **PPSTLTDDDA** **ARLLERLAFH** **KDGRRIDLGD** **DVGEGGARLS**  
501 **GGQVQKVELV** **RLMGVDVPAI** **VLETTSGLD** **PHSDTLGIAM** **LRERLGRRTT**  
551 **LVLITHRIAN** **VEAADQVLF**L **SGGRLVAAGP** HRRLVDT**CDE** YRTFWRRQPE  
601 PADATA

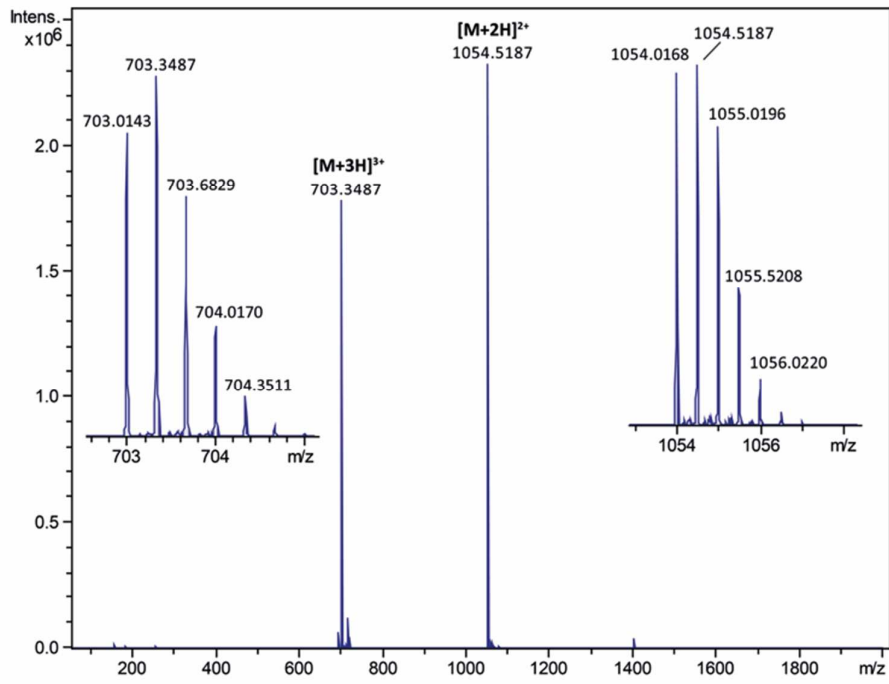
	<b>Score</b>	<b>Mass</b>	<b>Matches</b>	<b>Sequences</b>	<b>emPAI</b>
<b>gi 83655452</b>	1772	64859	55 (55)	24 (24)	5.8

**Supplementary Figure 8.** CapD characterization. a) CapD was extracted and purified in 0.03% DDM. CapD appears monodisperse in size exclusion (Superdex S200 10/300 column). The protein appears over 95% pure as judged by SDS-PAGE (inset). b) Purified CapD retains its basal ATPase activity in 0.03% DDM. c) The band from panel A was excized and analyzed by tryptic digest mass spectrometry. The band belongs to CapD with 52% peptide coverage.

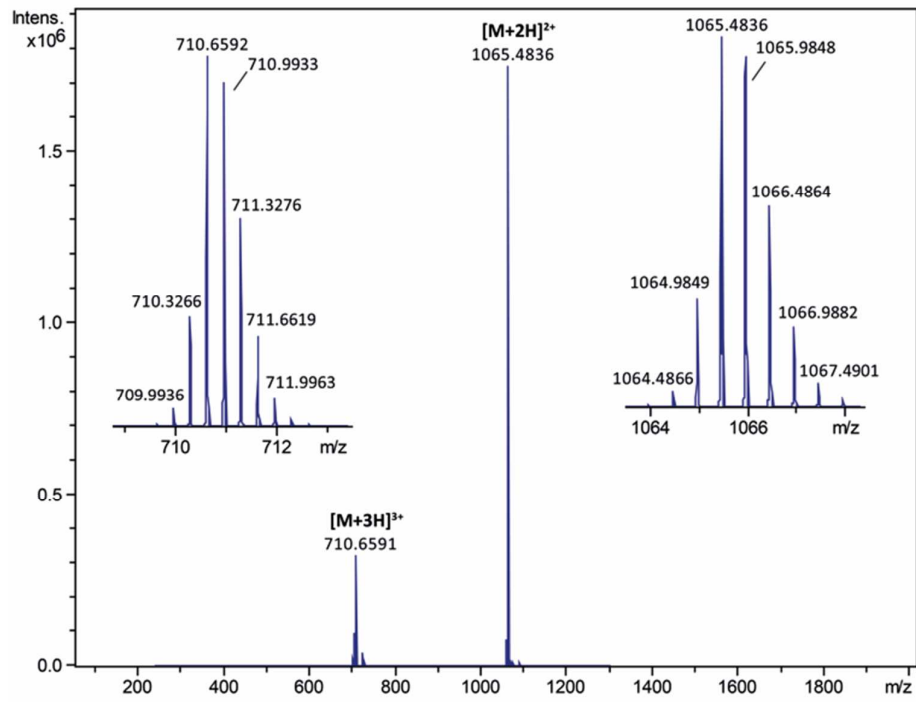


**Supplementary Figure 9.** Growth of drug-hypersensitive *E. coli*  $\Delta$ acrAB expressing empty pET28b plasmid in the presence (red) or in the absence (black) of MccJ25 (10  $\mu$ M). In the absence of McjD the cells cannot confer resistance to MccJ25 and cell growth is inhibited.

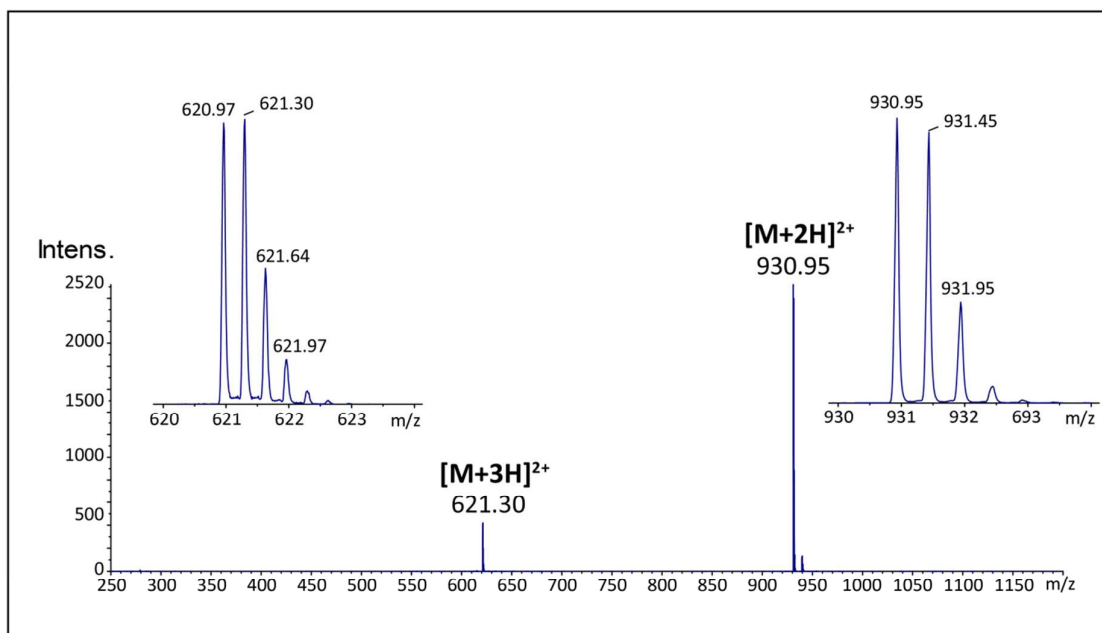
**a**



**b**



c



**Supplementary Figure 10.** ESI-MS spectrum of a) MccJ25, b)  $^{15}\text{N}$ -MccJ25 and c) MccJ25- $\Delta\text{FV}$ . All spectra have been acquired in positive ion mode.